VISCOUS EFFECTS IN TRANSONIC FLOW PAST AIRFOILS

J.J. Kacprzyński
National Research Council of Canada
Ottawa, Canada

Abstract

Contemporary supercritical airfoils are very sensitive to viscous effects. Even a very high Reynolds number wind tunnel test shows large differences compared with inviscid flow. Very often in the inviscid flow the lift coefficient is twice as high as in wind tunnel test, with completely different position and strength of shock waves and value of pitching moment.

In the paper the methods of calculations of viscous transonic flow are discussed and the results compared against results of the experiment. It is shown that the wind tunnel effects are difficult to separate and actually in order to have agreement between test and theory, one has to use not the theoretical results for free flow, but for viscous flow in the tunnel between porous walls.

List of Symbols

A	normalized angle of attack α/δ, also coefficient in nonlinear characteristics of the porous wall
B	empirical constant in enthaly and velocity law of the wall, also coefficient in nonlinear characteristics of the porous wall
C_p	pressure coefficient
C_L	lift coefficient
C_c	coefficient of chordwise force
C_{d_w}	wake drag coefficient
F	normalised airfoil shape function
H	wind tunnel height
K	transonic similarity parameter
M	Mach number
P	porosity parameter
c	chord of airfoil
f	airfoil shape function
m	coefficient in transonic similarity
n	coefficient in transonic similarity
x,y	cartesian coordinates
r,θ	polar coordinates in Sells plane
u	velocity
u_t	friction velocity
u*	Van Driest generalized velocity
$\tilde{y}$	transformed y coordinate
α	angle of attack
δ	relative airfoil thickness
δ_B	boundary layer thickness
δ^*	displacement thickness
γ	specific heat ratio
$\varkappa$	Karman constant (proportionality between mixing length and distance from airfoil surface)
ν_w	kinematic viscosity on surface
τ_w	shear stress on surface
ω	Coles law of wake function
$\tilde{\pi}$	Coles wake parameter
Γ	circulation
ϕ	perturbation velocity potential
Φ	velocity potential
Ω	relaxation parameter for boundary layer thickness

I. Introduction

In many cases the experimental pressure distribution and integrated aerodynamic coefficient for contemporary supercritical airfoils do not agree with the expected theoretical numbers. The disagreement is partly due to wind tunnel wall effects and partly due to viscous effects. Prediction of flight characteristics of an airfoil represents another difficulty. For many airfoils, particularly conventional ones, which behave very poorly at transonic speeds, and therefore are less sensitive to small perturbations of the flow parameters, the inviscid flow calculations performed for experimental values of Mach number and lift coefficients show good agreement with the experiment. Such comparisons for airfoil NACA 64A410 are given in References 1 and 2. The contemporary supercritical airfoils are very sensitive to variations of flow parameters and have very often completely different inviscid flow pressure distribution than the experimental one at the same Mach number and lift coefficient, particularly in the off-design flow condition. It makes the

prediction of flight characteristics of the airfoil very difficult; the flight test is difficult to perform and too late for the airplane designer.

The supercritical inviscid flow calculations are performed most economically (Ref. 3-5) by mapping the exterior of the airfoil to the inside of a circle (from physical plane to so-called Sells' plane) and by solving the full transonic flow equations with the relaxation method. Two methods of viscous flow calculations in the Sells plane are discussed and their drawbacks are indicated. These difficulties of calculation of the viscous flow in the Sells plane influenced the author to go back to the physical plane, although it is connected with an increase in the cost of calculations. The viscous flow calculations performed past shockless lifting airfoil No.2 show good agreement with wind tunnel results.

At present the viscous flow methods are being developed by many authors. Unfortunately the limited size of the present paper does not allow for review of these works, and therefore only the papers directly connected with the results presented are referred to.

II. Viscous Flow Calculations in the Sells Plane

The most elementary way of including viscous effects is by adding to the airfoil shape the displacement thickness of the boundary layer, recalculating the inviscid flow field by the modified airfoil, repeating the boundary calculations and so on until the convergent solution is obtained. Unfortunately in most cases the convergence is very poor and stopping the iteration at a certain point may show some improvement compared to inviscid flow calculations, but it does not represent the actual flow, because even a very small inaccuracy in boundary layer may have tremendous effects on the position of shock waves and aerodynamic characteristics of the airfoil.

The viscosity of the flow changes the flow past the airfoils by

1. changing the thickness of the airfoil
2. changing the camber
3. influence of wake

These three effects were tested in a simplified way in numerical experimentation (Ref.1). The supercritical inviscid calculations in the Sells plane are performed by marching along the surface of the airfoil from the leading edge to the trailing edge on the upper surface and on the lower surface independently. At each point of the surface a potential solution is solved in the column extending from the surface of the airfoil to the origin of the circle representing infinity. The boundary layer calculations in most methods are performed in the same way by marching with the integration from the leading edge towards the trailing edge. In the case of very thin boundary layer the boundary condition can be satisfied not at the edge of the boundary condition but on the surface of the airfoil itself. For relatively low lift coefficients, so that the camber of the airfoil is not changed, the change of the mapping function of the airfoil into the circle may be neglected. In this case the boundary layer changes only one boundary condition in the Sells plane from

$$\frac{\partial \Phi}{\partial r} = 0 \qquad \text{in inviscid flow} \qquad (1)$$

to

$$\frac{\partial \Phi}{\partial r} = -\frac{\partial \bar{\delta}^*}{\partial \theta}\,\frac{\partial \Phi}{\partial \theta} \qquad \text{for } r = 1 \qquad (2)$$

where $\bar{\delta}^*$ is the non-dimensional displacement thickness transformed into Sells plane.

Modifying in this way the boundary condition for the supercritical calculations and at each point of the surface of the airfoil evaluating the boundary conditions from a solution of the boundary layer, it is possible to obtain a convergent solution if the thickness of the boundary layer is under-relaxed. The process of iteration is nearly twice as slow as for inviscid flow calculation. Additional time is necessary for boundary layer calculation, so the total calculating time is up to three times longer than for the inviscid flow. In the above process the boundary layer was calculated using the Nash-MacDonald method (6). Some of the results of viscous flow calculations performed for airfoil NACA 65_1-213 are shown in Figures 1-2 with comparison against NACA flight results (7) and wind tunnel tests performed at NRC by Brown (1). The results of viscous flow calculations show better agreement with flight test and wind tunnel test than the inviscid calculations. This airfoil at these flow conditions represents a case where camber changes due to viscosity are small; airfoil itself has low camber, lift coefficient is low, so the boundary layer develops nearly symmetrically on both sides of the airfoil.

It is important to underline that this case represents a group for which the inviscid flow results calculated for experimental lift coefficients give good agreement with experiments. The viscous effects are mainly accounted for by a change of incidence of the airfoil and thickness effects have rather secondary influence.

As previously mentioned, calculated inviscid results do not agree with tests in many cases and small changes of incidence or Mach number in the calculations do not produce better agreement. In the process of including viscous corrections

it was discovered that the disagreements are caused by changes of the camber of the airfoil by boundary layer development, namely by decreasing it. Hence in such cases it is necessary to introduce modifications of the mapping function correcting the shape of the airfoil by a slightly modified boundary layer. It is a very difficult and computer time-consuming process and it follows that the viscous corrections cannot be treated as a small perturbation of inviscid flow any more. An example of experimental calculations for airfoil "x" is shown in Figure 3 in comparison with wind tunnel tests performed by Bowker (Ref.8) at Reynolds number 14.6×10^6. The viscous calculations were stopped after 1000 iterations with residue .00031, so the iterations had not fully converged. The viscous calculations were performed at Reynolds number $Re = 21.10^6$ and $M = .74$ and $\alpha = 0°$. The lift coefficient is .448 against .89 in inviscid flow. The experimental data with similar lift coefficient happens to be at lower Reynolds number. This comparison shows that the influence of the viscous effects is very significant and the viscous calculations show the right trend. It appears that in this case the boundary layer is separated on the lower surface in the region $.675 < x/c < .92$. On the upper surface the boundary layer separates at $x/c = .98$.

This example illustrates tremendous viscous effects for some airfoils. Unfortunaely, modifications of the mapping function (in calculated case about 100 times) is very computer time-consuming.

A modification of the mapping function in an empirical way as it was done nearly forty years ago for incompressible flow by Pinkertson (Ref.9) is rather impossible because too many parameters have an influence, namely Mach number, Reynolds number, lift coefficient and geometry of airfoil. Therefore, it may be more economical to perform the viscous flow calculations in the physical plane, where calculations of the mapping function are not necessary.

Another drawback of viscous flow calculations in the Sells plane, which hopefully may be eliminated in the future when more experience in viscous flow calculations is gained, is due to the fact that the poorest accuracy of the boundary layer calculation is near the trailing edge, and this region in the mapping to the Sells plane undergoes the largest transformation, which magnifies the errors. Any small change in the thickness of the boundary layer near the trailing edge may change completely the results of calculations particularly for rear camber airfoils.

Another difficulty is a treatment of wake and a tremendous influence of inaccuracy on results.

In the physical plane calculations these effects are easier to treat properly and it seems that they are less influential because they are not magnified by the mapping.

III. Viscous Flow Calculations in Physical Plane

Transonic flow calculations in the physical plane can be performed either using the time dependent method for full nonlinear problem as was done by Magnus and Yoshihara (Ref.10), or using the relaxation method for simplified small perturbation transonic equations, as was done by Murman and Cole (Ref.11), and Krupp (12).

The small perturbation approach is less computer time-consuming and simpler, therefore this method was used. First of all it was necessary to develop a computer program similar to Krupp's (12). Some modifications to Krupp's method were also introduced and they are described in Reference 13. The program solves a small perturbation transonic equation

$$\left[K-(\gamma+1)\phi_x\right]\phi_{xx}+\phi_{\tilde{y}\tilde{y}}=0 \tag{3}$$

where K is a transonic similarity parameter defined by a formula

$$K=\left(1-M^2\right)/\left(M^{2m}\delta^{2/3}\right) \tag{4}$$

with singular perturbation transformation of y coordinate and potential

$$\tilde{y}=\delta^{1/3}M^m y$$

$$\phi=\delta^{-2/3}M^n\Phi \tag{5}$$

with $n = 3/4$ and $m = \frac{1}{2}$.

The boundary conditions on the airfoil were originally used in a form

$$\left[\phi_{\tilde{y}}\right]_{u,l}=M^{n-m}\left(\left[\frac{dF}{dx}\right]_{u,l}-A\right) \qquad \text{at } \tilde{y}=\pm 0 \tag{6}$$

where $A = \alpha/\delta$ is a normalized angle of attack and

$$F_{u,l}(x)=f_{u,l}(x)/\delta \tag{7}$$

are functions specifying the shape of the airfoil and δ is relative thickness.

In the far field the analytical solution used by Krupp was used.

Pressure coefficients were determined from

$$C_p=\frac{\delta^{2/3}}{M^n}\tilde{C}_p \tag{8}$$

where

$$\tilde{C}_p=-2\phi_x$$

with lift coefficient determined by

$$C_L = \frac{\delta^{2/3}}{M^n}\,\Gamma \qquad (9)$$

where circulation Γ is calculated in process of iterations and accordingly the boundary conditions on the outer limit of the near field are updated.

From the numerical experimentation performed it appeared to be useful to introduce Riegel's factor by dividing the boundary condition (6) by

$$\sqrt{1+(f'_{u,l})^2}$$

It corrects significantly the pressure distribution on the forward part of the airfoil.

The results of the modified small perturbation method were compared against the practically exact results of calculations of airfoil NACA 0012 (Ref.3).

For illustration pressure distribution at $M = .8, \alpha = 1°$ is shown in Figure 4. The position of the shock on the upper surface differs by about 3% of chord, on the lower surface it is nearly identical. The lift coefficients differ by about 10%. So using the small perturbation method for viscous flow calculations one has to accept that it is rather impossible to have better accuracy.

The cost of inviscid calculations in the physical plane is nearly 100 times higher than for the same in the Sells plane, but taking into account that during the viscous calculations one has to perform mapping over 100 times, the cost of calculations of the viscous flow in the physical plane may be comparable to the cost of calculations in the Sells plane. Some attempts to reduce the cost of calculations using methods of acceleration of convergence based on Shanks-Aitken method, have been already undertaken by Martin and Lomax (Ref.14) and Hafez and Cheng (Ref.15).

In the viscous flow calculations the calculation of the boundary layer was coupled with calculations of the outer inviscid flow. In the region of the attached flow the boundary layer was calculated using Nash-MacDonald (Ref.6) method. In the region behind the first separation the Alber (Ref.16, 17) method was used. It employs, modified to compressible adiabatic flow, Coles' law of the wall and law of the wake

$$\frac{u}{u_\tau} = \frac{1}{\kappa}\ln\left(\frac{y\,u_\tau}{\nu_w}\right) + B + \frac{\tilde{\pi}}{\kappa}\,\omega\left(\frac{y}{\delta_B}\right) \qquad (10)$$

with $\kappa = .41$, $B = 5$ and $\omega(y/\delta_B)$ given by Cole's wake profile.

The calculated displacement thickness was added to the shape of the airfoil in under-relaxed mode, updating the shape of the airfoil every 10 iterations.

Hence in the viscous flow the airfoil shape function were modified to

$$\bar{f}_{u,l}(x) = f_{u,l}(x) + (1-\Omega)\,\delta_i^*(x) + \Omega\,\delta^*_{i+10}(x) \qquad (11)$$

where under-relaxation parameter in order to secure stability of solution has to be smaller than 0.5 and δ_i^* and δ^*_{i+10} are displacement thickness after i and i+10 iterations. The shape function and far field boundary conditions were updated every 10 iterations.

IV. Wind Tunnel Wall Effects

Till now the only published method for calculations of wind tunnel wall effects is Murman's method (Ref.18). In this method the solution in near field (Fig.5) is obtained numerically solving a small perturbation transonic equation with the relaxation method. The near field is bounded from the top and bottom by porous wind tunnel walls, with boundary conditions

$$\frac{\partial \phi}{\partial \tilde{y}} = -\tilde{P}\,\frac{\partial \phi}{\partial x} \qquad \tilde{y} = \pm\tilde{H} \qquad (12)$$

where $\tilde{P}$ - porosity parameter was constant.

Near field in front of the airfoil and back behind the trailing edge is bounded by analytical far field solution.

This method was modified (Ref.19) using similar changes to ones introduced in Reference 13 to Krupp's method (Ref.12).

It was known long ago (Lukasiewicz - Ref.20) that the porous walls behave differently for inflow than for outflow and actually the wall characteristics are nonlinear, or at least second order function of ϕ_x (Berndt, Ref.21) as shown in Figure 6

$$\phi_{\tilde{y}} = A\,\phi_x + B\,\phi_x^2$$

where A and B are certain coefficients having different values for $\phi_x > 0$ (suction - inflow) and $\phi_x < 0$ (outflow). Therefore the Murman method was modified so that it allows for any wall characteristics given in analytical or numerical formulas (Ref.22). One of the ways for calculation of analytical far field solution for arbitrary wall characteristics is given in Reference 22.

The numerical studies performed of the flow past several airfoils indicate that the flow field in the wind tunnel is quite different from the flow field in free air, and that the two sought for magic values ΔM and $\Delta\alpha$ eliminating the wall effects do not exist.

The applied wall correction may decrease the wall effects but it is rather impossible

to eliminate them completely. As an illustration some results of supercritical flow field past airfoil NACA 0012 at M = .8, α = 1°in free air and between walls with porosity P = 1 for Cp < 0 and .33 for Cp > 0 for H/c = 5.08 are shown in Figure 7. The difference between lift coefficient is 15%. The printed numbers are the truncated values of the local angle of flow. A second example (Fig.8) is a subcritical inviscid flow field past airfoil NACA 64A410 at M = .5 for C_L = .6 calculated in free flow (α = 1.6) and in the wind tunnel (α = 2.24°) with porosity P = 1.5 for C_p < 0 and .5 for CP > 0.

The calculations performed show that the flow fields in free air and in the wind tunnel are different and changing ΔM and $\Delta\alpha$ only partially the differences can be eliminated.

V. Studies of the Viscous Flow past Shockless Lifting Airfoil No.2

Transonic two-dimensional testing of airfoils is performed in NRC in the 5 ft x 5 ft high Reynolds number wind tunnel with two-dimensional 15" x 60" insert (Fig.9). The model of airfoil is supported at two ends by two three-component balances which rotate with model and record also the incidence. Data system makes it possible to use a fast scanning pressure measuring and a fast traversing side wall mounted wake rake. Simultaneous force, wing pressure and wake traverse measurements are made. The pressure-measuring system allows the scanning of 80 surface pressures and full wake survey in 2.5 seconds. The Mach number control system is capable of holding the test Mach number to within ±0.001 during a run. The top and the bottom walls of the test section have 20.5% porosity (and it can be reduced if desired). In the 2-D insert design special attention was paid to the control of sidewall boundary layer. Besides the boundary layer bleeding slots located at the 2D insert contraction, removing the boundary layer from the 5 x 5 ft wind tunnel walls upstream of the test section, around the model location sidewalls are made of porous material allowing distributed suction. It allows for very effective removal of side wall boundary layer near the model but makes it impossible to use the schlieren system for observation of shock waves and boundary layer on the model. At high Reynolds numbers the boundary layer is very thin and therefore there is no possibility to measure the velocity profile. So from the experimental point of view we know practically nothing about the boundary layer. Only the "quick-look" raw data system gives some information. Namely during the scanning of the pressure distribution on the model the "raw signals" are displayed on x-y plotter (Fig.10). The mean value of the pressure signal is plotted as a small horizontal line, and time dependent value is plotted as a vertical line. If the signal corresponds to steady pressure on the upper surface-it is printed a dot; if on the lower surface-it is printed as a triangle with correct value in the upper corner. These plots make it possible to study steadiness of the flow, repeatability of results, indicate region of separations, etc.

The lack of possibility of direct measurements of boundary layer on an airfoil and lack of data about boundary layer developments at very high Reynolds numbers stimulated us to perform the following experiment with shockless lifting airfoil No.2 designed by Frances Bauer and P.R. Garabedian. It is a 15.1% thick airfoil designed for shockless flow at M = .75 with C_L = .667. The design shape of the airfoil, design pressure distribution and characteristics in the supersonic region are shown on the left side of Figure 11. For the design pressure distribution the boundary layer was calculated at Reynolds number 20.10^6 using Nash-MacDonald method. The displacement thickness of the boundary layer was subtracted from the theoretical shape producing a thinner airfoil (dotted line B). This thinner contour was used for model manufacturing and both inviscid and viscous flow calculations.

It was expected that if the boundary layer calculations were correct, then in the flow at Re = 20.10^6 the design pressure distribution indicated on the left side of Figure 11 should be obtained in the wind tunnel tests. The inviscid pressure distribution calculated for the thinner airfoil B are shown on the right side of the Figure 11. It has completely different character than the design pressure distribution, with supersonic region terminated by a very strong shock wave. The maximum local Mach number was M_{loc} = 1.68, so the isentropic approximation is not valid any more. Supercritical airfoils with such strong shock waves are usually rejected. The calculated inviscid flow lift coefficient C_L = 1.183 is nearly twice higher than the design one at the same angle of attack α = 0°. The comparison of these two pressure distributions illustrates how important in some cases the viscous effects can be. Differences of this magnitude have been observed for many airfoils in supercritical flow. In many cases the inviscid flow calculations show very strong shock waves while in the experiments the shocks are weaker and the lift coefficients are much smaller.

In performed wind tunnel tests (23) the design pressure distribution was not obtained, which is not surprising because it was known a priori that the Nash-MacDonald method used for the boundary layer calculations is not very accurate. Unfortunately none of the existing boundary layer methods is accurate in the transonic regime. For the theoretical design case it

was not possible to obtain a shockless flow, and the experimental lift coefficient was much lower than expected. After very careful experimentation it was possible to find two regions of shockless or nearly shockless flow at much higher Mach numbers, one nearly shockless flow at M = .767 with C_N = .585 and the second one with much smoother termination of the supersonic region at M = .778 and with C_N = .494, (Fig.12). To illustrate how sensitive the shockless flow is to small perturbations of the flow parameters, some pressure distributions are presented in Figure 13. For the same Mach number M = .778 pressure distributions at the end of the supersonic region are shown at three incidences different from one another by .03°. The middle one corresponds to near shockless conditions, changing the angle of attack by only .03° in one or the other direction causes the appearance of shock waves. The strength of the shock wave increases rapidly with change of the angle of attack.

Although the absolute value of angle of attack may be determined with difficult to estimate accuracy, the relative change of angle of attack is measured very accurately. This strong change of the pressure distribution for such small change of angle of attack explains also the very strong viscous effects and strong effects of errors in calculations of boundary layer near the design conditions.

The shockless lifting airfoil No.2 was tested very extensively for Reynolds number in the range from 14.10^6 up to 37.10^6. Most of the experimental results are presented in Reference 23.

The experimental results obtained do not agree with inviscid flow calculation even performed for experimental lift coefficients.

Many other contemporary airfoils show similar disagreements and therefore it was thought to be useful to explain the difference between the theory and experiment.

Let us for example take some experimental results of the flow past this airfoil at the same Mach number and angle of attack but at four different Reynolds numbers ranging from 14.10^6 up to 28.10^6. The experimental pressure distributions are shown in Figure 14. In order to explain the experimental results the following studies were performed. In the previous studies of the flow past a symmetrical shockless Boerstoel airfoil 0.11 - 0.75 - 1.375 (Ref.24-26) it was discovered that the flow in the wind tunnel is not parallel to the top and bottom walls but has some angularity of the order -0.3°* in this region of Mach numbers. Probably this angularity is not uniform, but it is difficult to detect it. Hence from the experimental angle of attack 1.96° 0.3° was subtracted.

Calculations of the inviscid flow at angle of attack 1.66° in free air, have no sense, the lift coefficient is ~2; ~400% higher than experimental one. Calculations of the inviscid flow for experimental lift coefficients also have no sense, pressure distribution is completely different. Hence it is obvious that one has to use wind tunnel wall corrections or calculate the flow past airfoil between porous wind tunnel walls. Unfortunately there is no method for realistic wind tunnel wall corrections, therefore the transonic flow field between the porous wind tunnel walls was calculated.

First of all the inviscid flow was calculated at M .762, α = 1.66° for porosity P .355**.

The results of calculations at α = 1.66° are shown in Figure 15. Lift coefficient is between 50 and 100% higher than the experimental ones shown in Figure 14, which is not surprising.

It appears that the correction of angularity of the flow used is quite good. At lower angle of attack the suction behind the leading edge on the upper surface is too small, for higher α the suction on the lower surface is too small.

Using the results of the inviscid flow calculations between porous walls as a starting point for viscous flow calculations, the four experimental cases were calculated with the same porosity 0.355 and H/c = 6 and obtained pressure distributions are compared against experiment in Figures 16 - 19. The agreement is very good although far from perfect. In all four cases the experimental pressure coefficients just behind the leading edge both on the upper and the lower surface are lower than calculated. It means that the boundary layer must be thicker; may be there exist local separation bubbles not indicated theoretically. The "quick-look" raw data plots are presented in Figures 20-23. In Figure 22 two "crosses" on the upper surface behind the leading edge indicated oscillations of pressure (vertical lines) may be explained only by local separation.

* decreasing angle of attack

** It appears from numerical experimentation that in order to calculate flow field for high values of porosity parameters, one has to start with small values and change them gradually to the desired values, otherwise it is difficult to obtain the stable solution. From the calculated cases it appears that for large H/c the pressure distribution on the airfoil is not very sensitive to the change of porosity for high porosity parameters. Because of high cost of calculations the calculation for higher values of porosities were not performed.

The experiment at Re = 14.10^6 (Figure 16) agrees very well with theory, the position of the shock wave on the upper surface is identical, the theoretical suction on the lower surface is too low, also pressure in the region of rear camber is too high. The lift coefficient differ only 8% (only, because as it was shown for calculation of NACA 0012 the difference between the exact calculations and small perturbation was about 10%).

The results for the remaining three Reynolds numbers (Figures 17-19) show poorer agreement, lift coefficients differ 18 to 23%. In all cases theoretical suction in the lower surface is too small. In order to examine the influence of the pressure distribution on the boundary layers development, the boundary layer for four experimental cases were calculated for experimental pressure distributions and compared against results of boundary layer calculations for viscous flow calculations, (Fig. 24-31). Boundary layers on the upper surface (Fig. 24-27) show extremely good agreement; on the lower surface agreement in the region of the rear camber is poor. On the bottom of the figures the calculated regions of separation are indicated. Quick data look (Figures 20-23) show actually much larger regions of separations (crosses on upper surface) particularly for Reynolds numbers $24.8.10^6$ and 28.10^6. The vertical lines indicate oscillations of pressure. The physical separation is an unsteady phenomenon, the theoretical model assumes "steady" separation, which is a large simplification of the true flow and it may explain the discrepancies between the theory and experiment. Also it is known that the Coles wake model does not predict correctly the separation. In order to check experimentally the unsteadiness of flow and repeatability of results some tests were repeated, by repeating all the recordings during the same wind tunnel run for practically the same Mach number and angle of attack. Raw data quick-look results of four scans at Reynolds number $24.8.10^6$ are shown in Figure 22. The oscillations are shown behind the shock wave on the lower surface behind the leading edge. Also separation on the forward part of the upper surface (two crosses) are indicated. After data reductions the results are shown in Figure 32. The test data for those four scans are contained in Table 1.

Raw data "quick-look" plot for two scans at Re = 28.10^6 is shown in Figure 23 showing large oscillations behind the shock wave.

VI. Conclusions

The presented studies of the viscous flow past shockless lifting airfoil No.2 show that in order to remove the disagreement between the experiment and theory, the theoretical calculations must treat not the free air flow, but the flow between porous wind tunnel walls. The viscous calculations reduce the difference between the theory and experiment to 20%, which may be considered as a small and acceptable difference, because the difference between the exact inviscid calculations in the Sell's plane and small perturbation theory in the physical plane are of the order of 10%.

It is very difficult to explain completely the difference between the experiment and viscous flow calculations. One reason of discrepancy is the assumed model of steady flow even in the separated region, the experiment shows that the flow is unsteady, but calculations of unsteady viscous flow cannot be performed because of the cost. It is also difficult to judge what is more correct - the experimental data or the calculated data, because it is extremely difficult to estimate the accuracy of the test and influence of many small effects being usually neglected. The calculation of the boundary layer is also far from perfect. The assumed model of the flow between porous wind tunnel walls is also very simplified.

Another thing not treated properly is wake (theoretically it was considered as straight line of discontinuity of potential). Actually wake has curvature, but taking it into account and solving it as a near wake problem is very expensive. Also, the assumption that the flow in the wind tunnel has uniform angularity may be too simplified. All these small inaccuracies of representation of actual flow added together produce error between the theory and experiment of 20%. Unfortunately it does not seem possible to reduce this error, because the cost of calculations is already too high for practical calculations. It may happen that for some airfoils or for some flow parameters, as in the case of the experiment at Re = 14.10^6, the discrepancy between theory and experiment may be smaller, but it is rather more of a coincidence than a general expected rule.

The calculated flow field between the wind tunnel walls differs significantly from the free flow, therefore even a very high Reynolds number test may not represent the free flow past the airfoil at the same Reynolds number. It seems that the only fully reliable method of prediction of free flight characteristics of the airfoil would be from the theoretical viscous method, identical to that used for explanation of wind tunnel results.

Too little is known both experimentally and theoretically about boundary layer development at very high Reynolds number. For the flight flow parameter, with relatively weak shock waves on the upper surface, not causing buffet onset or full

separation between the shock wave and trailing edge, the development of the boundary layer on the lower surface seems to be more critical causing separation at the beginning of the region of rear camber and decrease of lift.

References

1. Kacprzynski, J.J., Drag of supercritical airfoils in Transonic Flow, AGARD-CP-124, April 1973.

2. Ohman, L.H., Kacprzynski, J.J., Brown, D., Some Results from Tests in the NAE High Reynolds Number Two-Dimensional Test Facility on Shockless and other Airfoils, ICAS Paper No.72-33, 1972, also Canad. Aeronautics and Space Journal, Vol.19, No.6, 1973.

3. Kacprzynski, J.J., Extension of Sells' Method to Supercritical flow Calculations. (not published)

4. Kacprzynski, J.J., Theoretical Studies of the Inviscid Transonic Flow Past Airfoil NACA 0012. NRC, LTR-HA-9, January 1973.

5. Kacprzynski, J.J., Theoretical Studies of Inviscid Transonic Flow Past Two Boerstoel Shockless Airfoils, the Symmetrical 0.11-0.75-1.25 and a Lifting Airfoil. NRC, LTR-HA-17, July 1973.

6. Nash, J.F., MacDonald, A.G.J., The Calculations of Momentum Thickness in a Turbulent Boundary Layer at Mach Number up to Unity, ARC-CP No.963, 1967.

7. Brown, H.H., Clousing, L.A., Wing Pressure Measurements up to 0.866 Mach Number in Flight on Jet-Propelled Airplane, NACA TN1181, 1947.

8. Bowker, A.J., private communication.

9. Pinkerton, R.M., Calculated and Measured Pressure Distribution over the midspan section of the NACA4412 Airfoil, NACA Report 563, 1936.

10. Magnus, R., Yoshihara, H., Steady Inviscid Transonic Flows over Planar Airfoils, NASA CR No.2186, 1972.

11. Murman, E.M., Cole, J.F., Calculations of Plane Steady Transonic Flows, AIAA Journal, Vol.9, pp.114-121, 1971.

12. Krupp, J.A., The Numerical Calculation of Plane Steady Transonic Flows Past Thin Lifting Airfoils, Boeing Sci., Res.Lab.Rep. D180-12958-1, Seattle, 1971.

13. Kacprzynski, J.J., Couet, B., Analysis of Two-Dimensional Transonic Flow Calculations using small Disturbance Approximations, NRC, LTR-HA-21, April 1974.

14. Martin, D.E., Lomax, H., Rapid Finite-Difference Computation of Subsonic and Transonic Aerodynamic Flows, AIAA Paper 74-11, 1974.

15. Hafez, M.M., Cheng, H.K., On Acceleration of Convergence and Shock-Fitting in Transonic Flow Computations, Memorandum, Dept. of Aerospace Engineering, Univ. of Southern Calif., Los Angeles, 1973.

16. Alber, I.E., Bacon, J.W., Masson, B.S., Collins, D.J., An Experimental Investigation of Turbulent Transonic Viscous-Inviscid Interactions, AIAA Paper 71-565, 1971.

17. Alber, I.E., Coates, D.E., Analytical Investigations of Equilibrium and Nonequilibrium Compressible Turbulent Boundary Layers, AIAA Paper 69-689, 1969.

18. Murman, E.M., Computation of Wall Effects in Ventilated Transonic Wind Tunnels, AIAA Paper, No.72-1007, 1972.

19. Kacprzynski, J.J., Couet, B., Analysis of Two-Dimensional Small Perturbation Transonic Flow Between Porous Wind Tunnel Walls, NRC report in preparation.

20. Lukasiewicz, J., Effects of Boundary Layer and Geometry on Characteristics of Perforated Walls for Transonic Wind Tunnels, Aerospace Engineering, April 1961.

21. Berndt, S., Private communication, April 16, 1974.

22. Kacprzynski, J.J., Small Perturbation Flow Field Between Porous Walls with Nonlinear Porosity, NRC report in preparation.

23. Kacprzynski, J.J., Wind Tunnel Test of a Shockless Lifting Airfoil No.2, NRC Report LTR-HA-5x5/0067, Oct. 1973.

24. Kacprzynski, J.J., Analysis of the Wind Tunnel Flow Angularity and Repeatability of Test Result in Supercritical Condition, NRC, Lab Memo HSA-55, 1971.

25. Kacprzynski, J.J., Wind Tunnel Investigation of the Boerstoel Shockless Symmetrical Airfoil 0.11-0.74-1.375, NRC Report 5x5/0061, 1972.

26. Kacprzynski, J.J., Analysis of the Flow Past Boerstoel Shockless Symmetrical Airfoil 0.11-0.75-1.375, NRC, LTR-HA-10, January 1973.

TABLE 1

SCAN	1	2	3	4
M	.779	.770	.771	.771
Re.10^{-6}	24.78	24.80	24.80	24.68
$\alpha°$	1.983	1.981	1.981	1.981
C_n-pressure	.516	.520	.517	.524
C_n-balance	.511	.510	.509	.509
C_c-blanace	.00865	.00872	.00875	.00886
wake 1 central	.01312	.01261	.01135	.01237
wake 2	.01238	.01236	.01160	.01184
wake 3	.00979	.01235	.01097	.01147
wake 4 (near wall)	.00928	.01165	.01478	.01162
weighted average	.01072	.01209	.01267	.01175

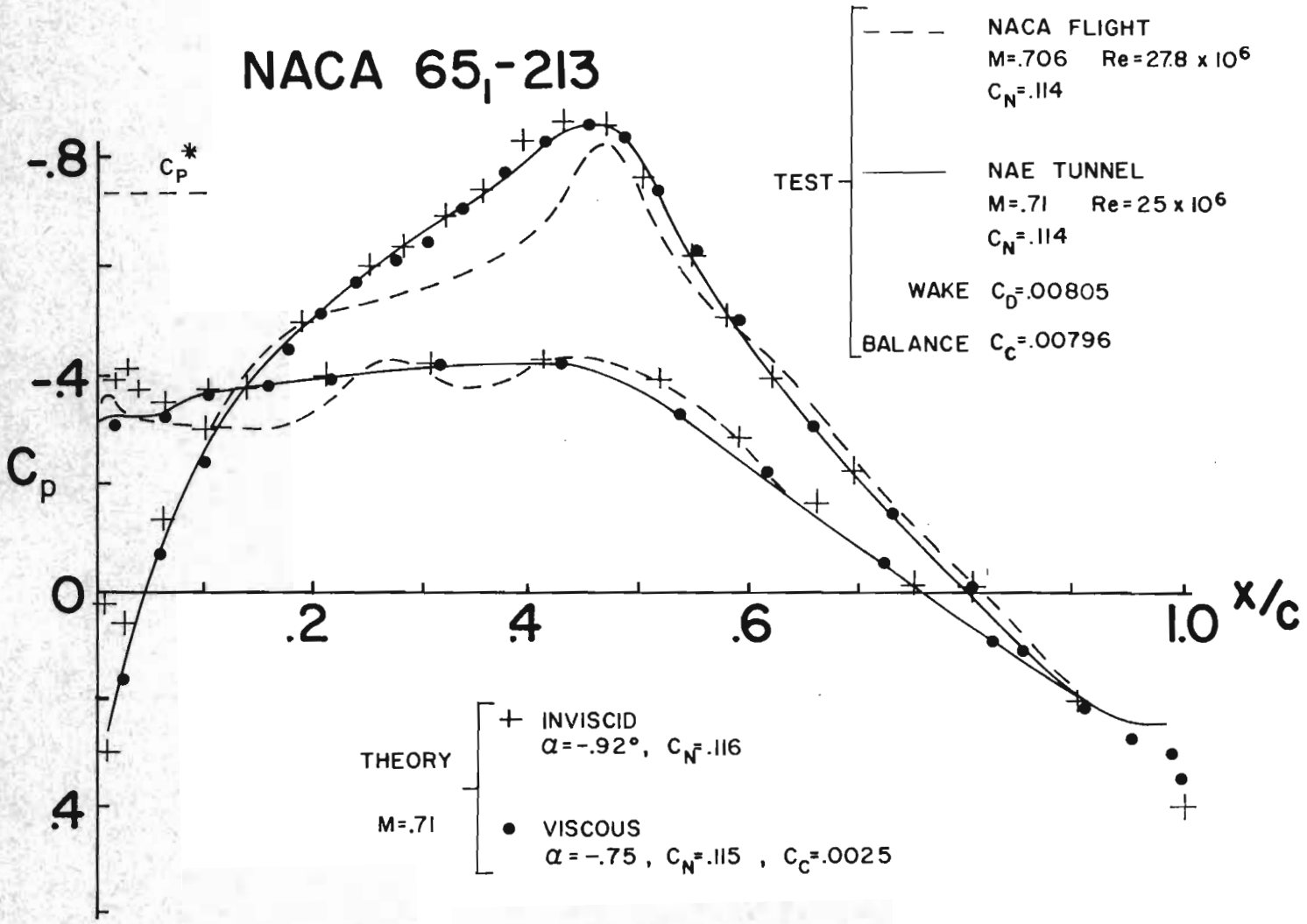

FIGURE 1 PRESSURE DISTRIBUTIONS ON AIRFOIL NACA 65_1-213

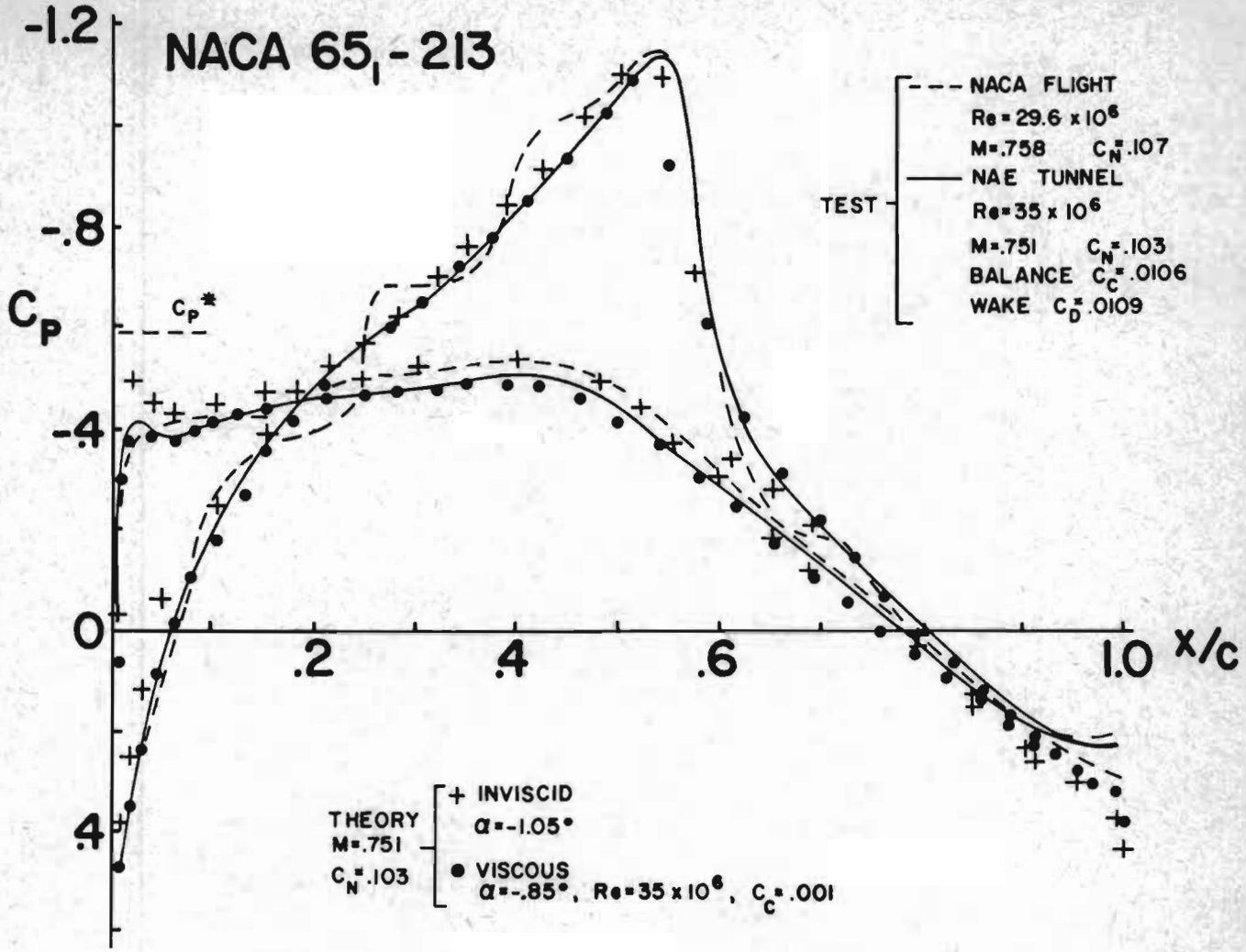

FIGURE 2 PRESSURE DISTRIBUTIONS ON AIRFOIL NACA 65_1-213

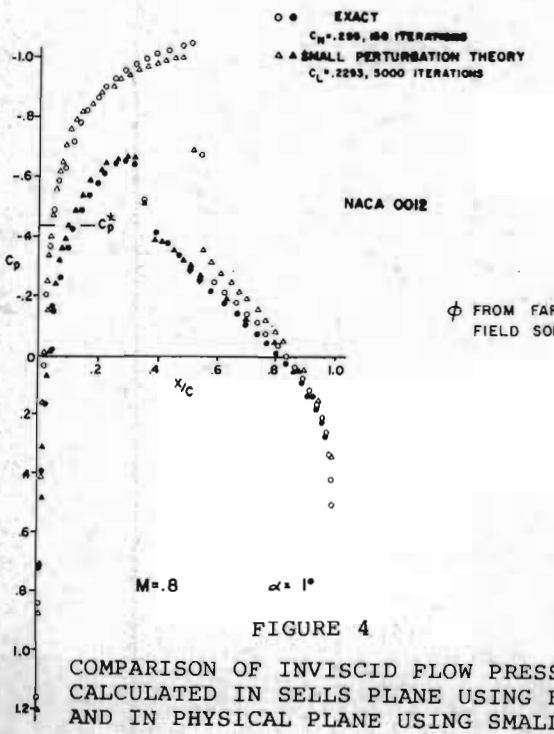

FIGURE 4

COMPARISON OF INVISCID FLOW PRESSURE DISTRIBUTION CALCULATED IN SELLS PLANE USING EXACT EQUATIONS AND IN PHYSICAL PLANE USING SMALL PERTURBATION THEORY

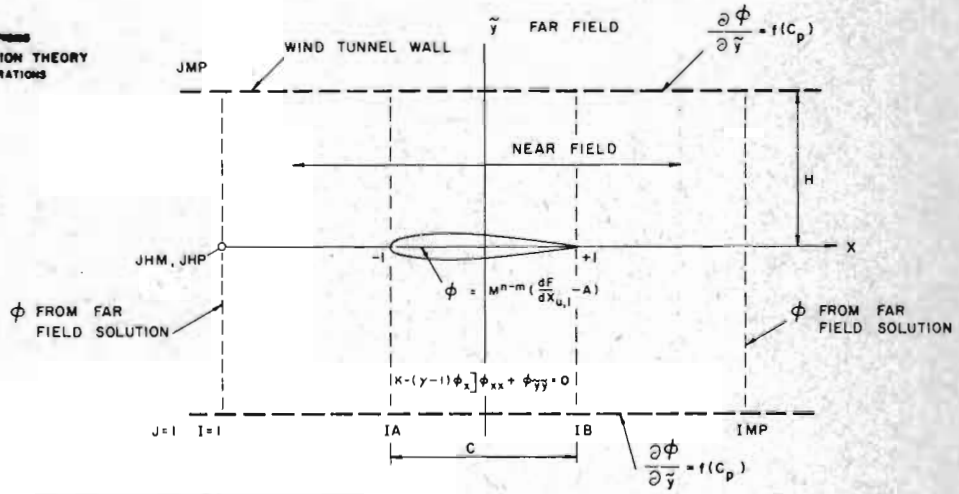

FIGURE 5

REPRESENTATION OF THE PROBLEM OF THE FLOW PAST AIRFOIL BETWEEN POROUS WIND TUNNEL WALLS

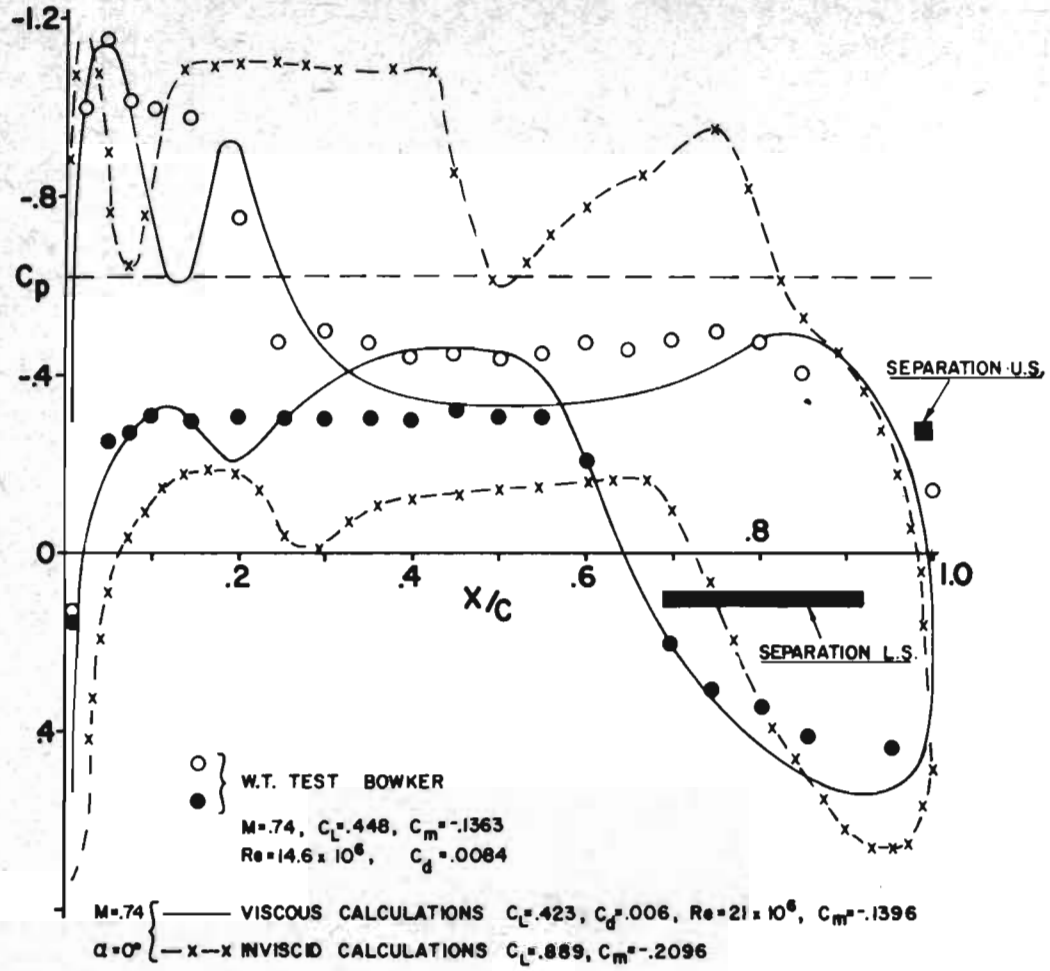

FIGURE 3 PRESSURE DISTRIBUTION ON SUPERCRITICAL AIRFOIL X

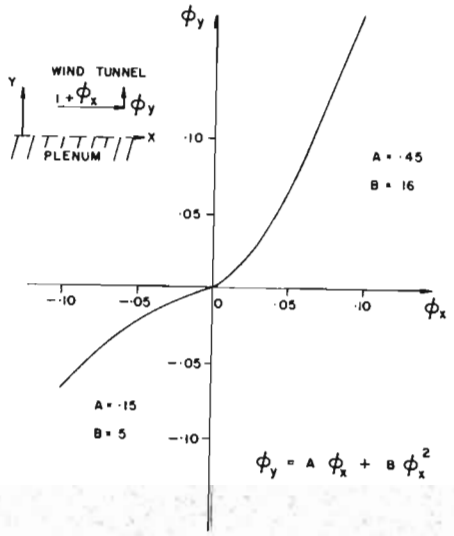

FIGURE 6 EXAMPLE OF NONLINEAR CHARACTERISTICS OF THE POROUS WIND TUNNEL WALL

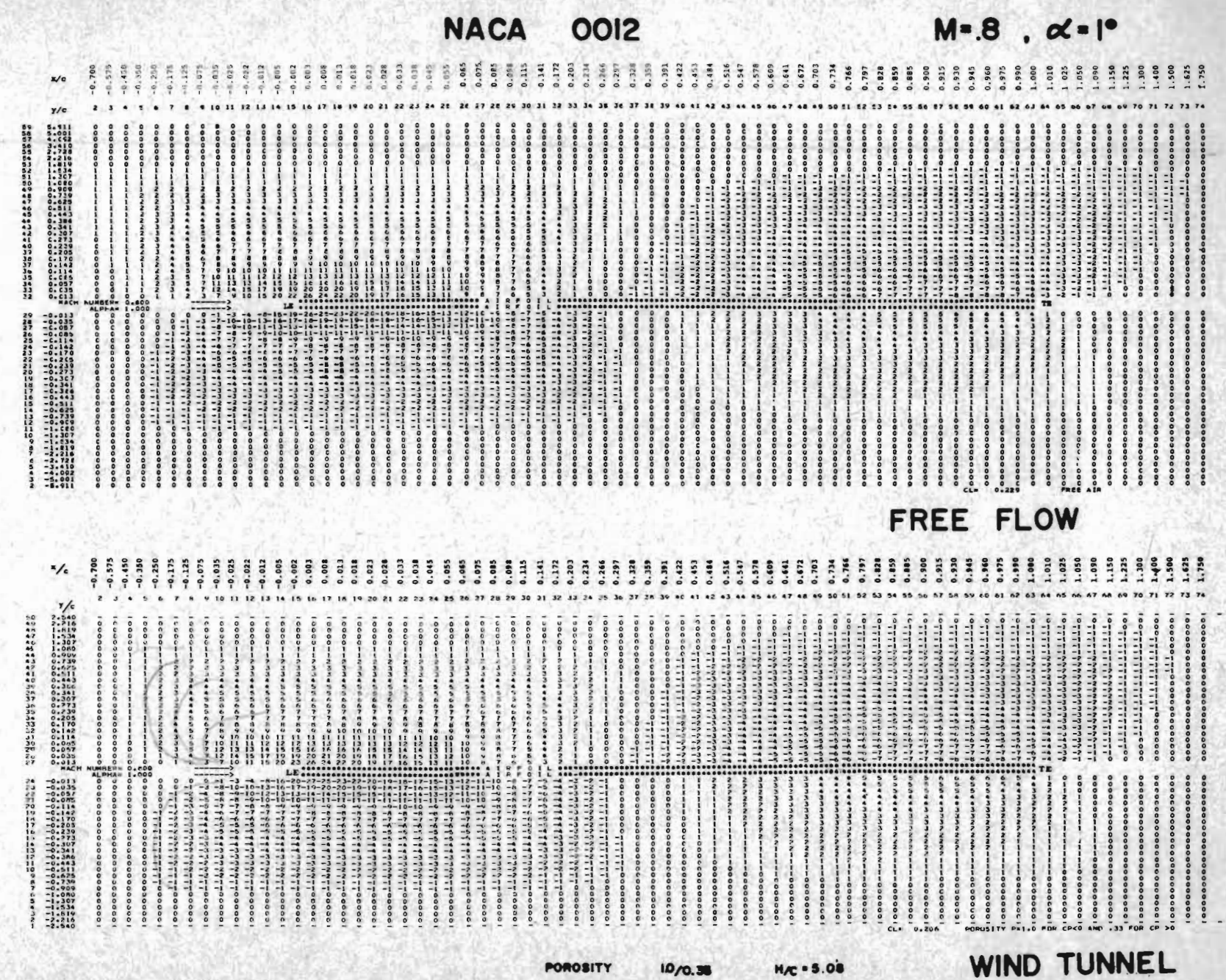

FIGURE 7 COMPARISON OF SUPERCRITICAL FLOW FIELDS PAST AIRFOIL NACA 0012 AT M = .8, α = 1° (PRINTED ARE TRUNCATED VALUES OF ANGLES OF THE FLOW IN DEGREES)

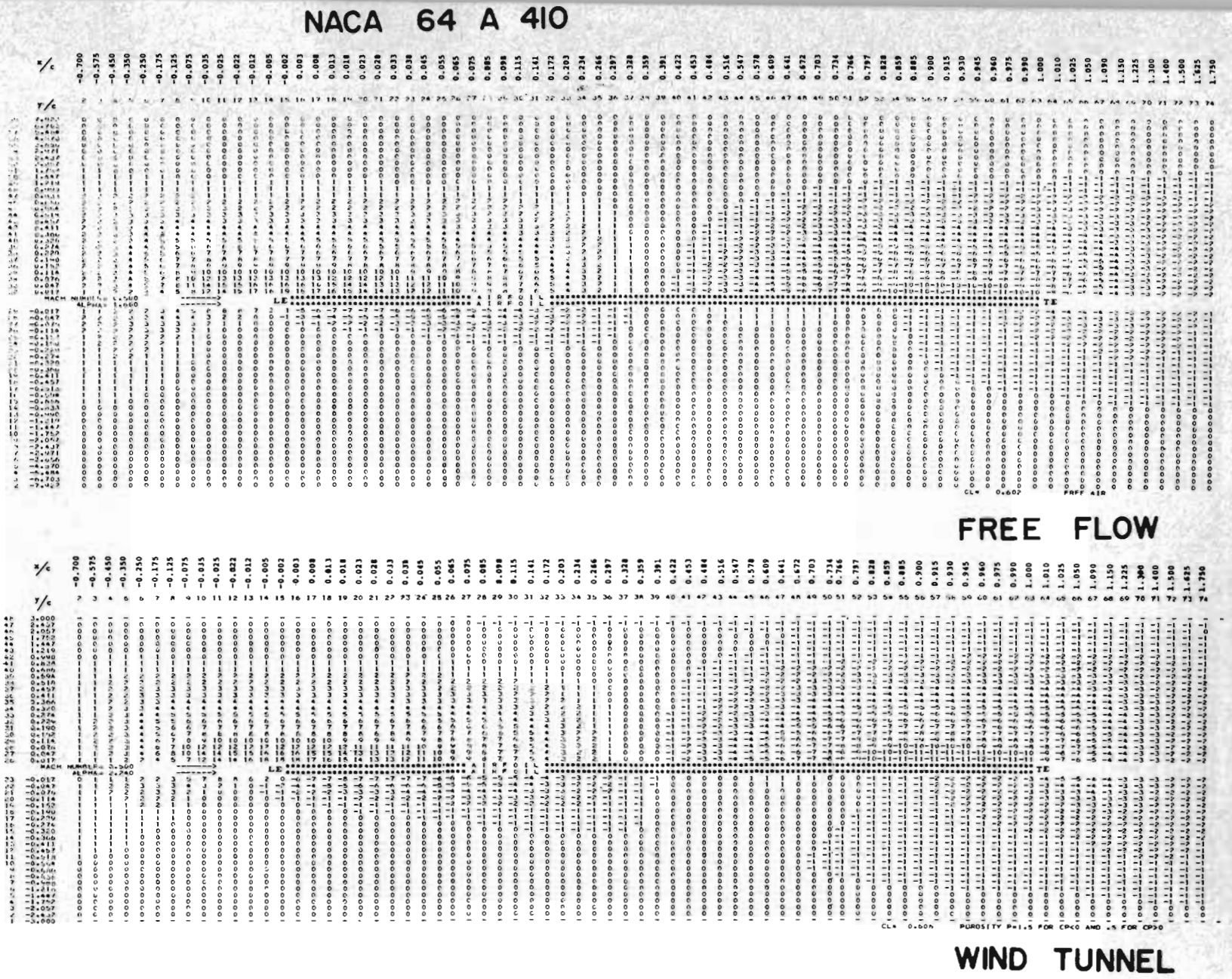

FIGURE 8 COMPARISON OF SUBSCRITICAL FLOW FIELDS PAST AIRFOIL NACA 64A410 AT M = .5 AND C_L = .6 (PRINTED ARE TRUNCATED VALUES OF ANGLES OF FLOW IN DEGREES)

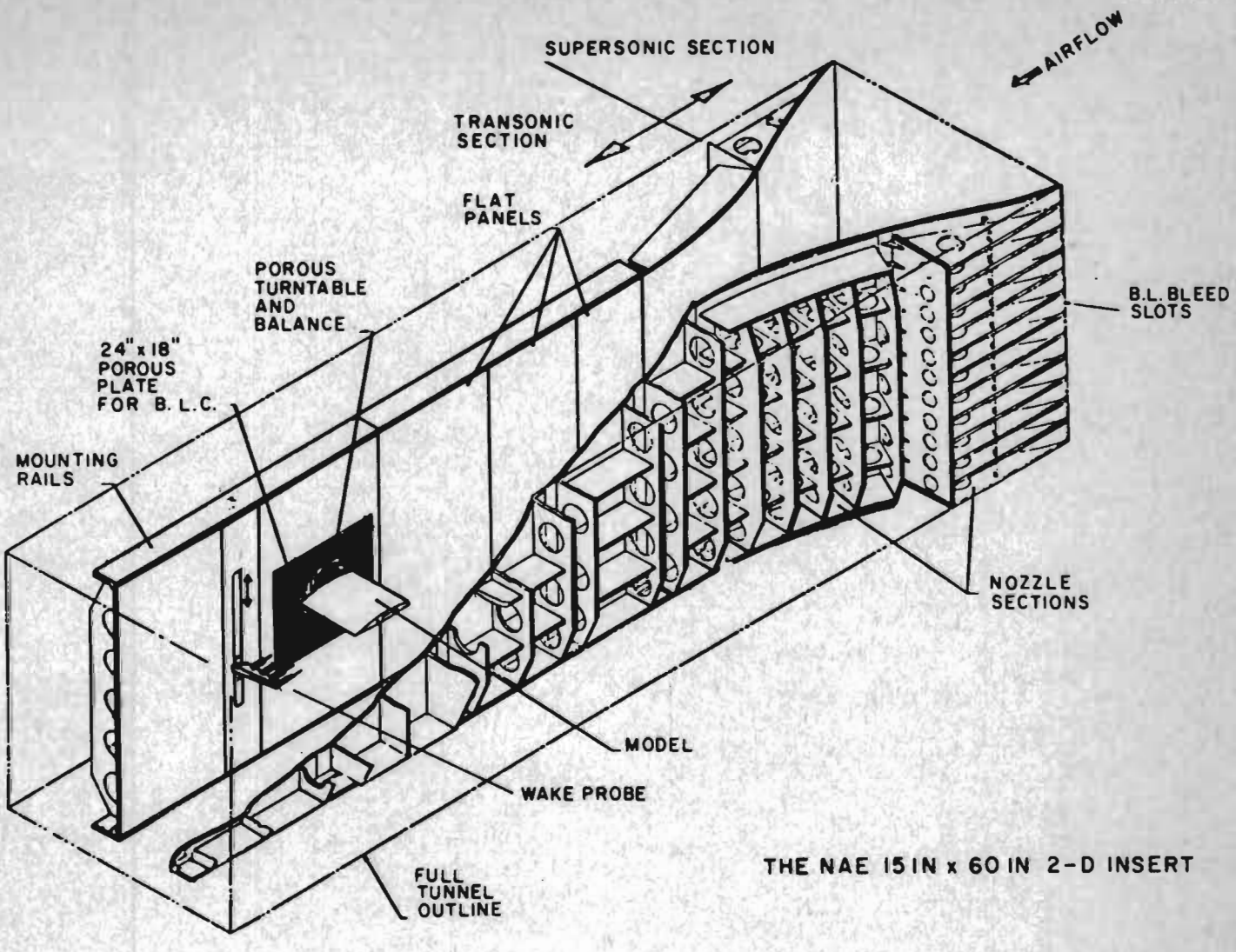

FIGURE 9 NRC HIGH SPEED WIND TUNNEL

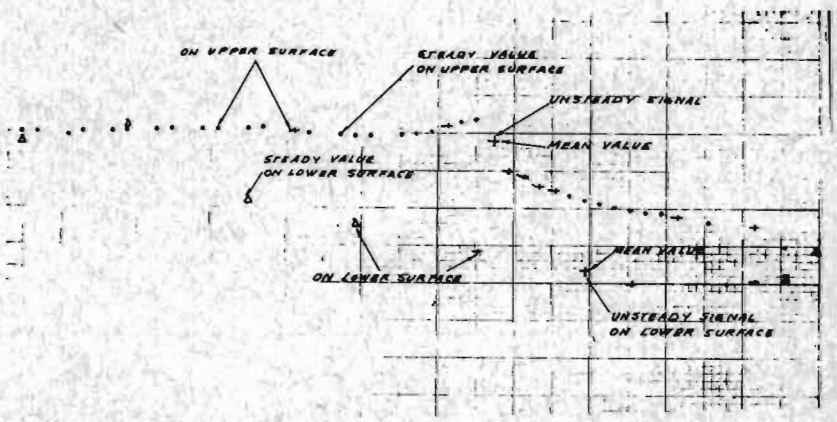

FIGURE 10 EXPLANATION OF "QUICK-LOOK" RAW DATA PLOT

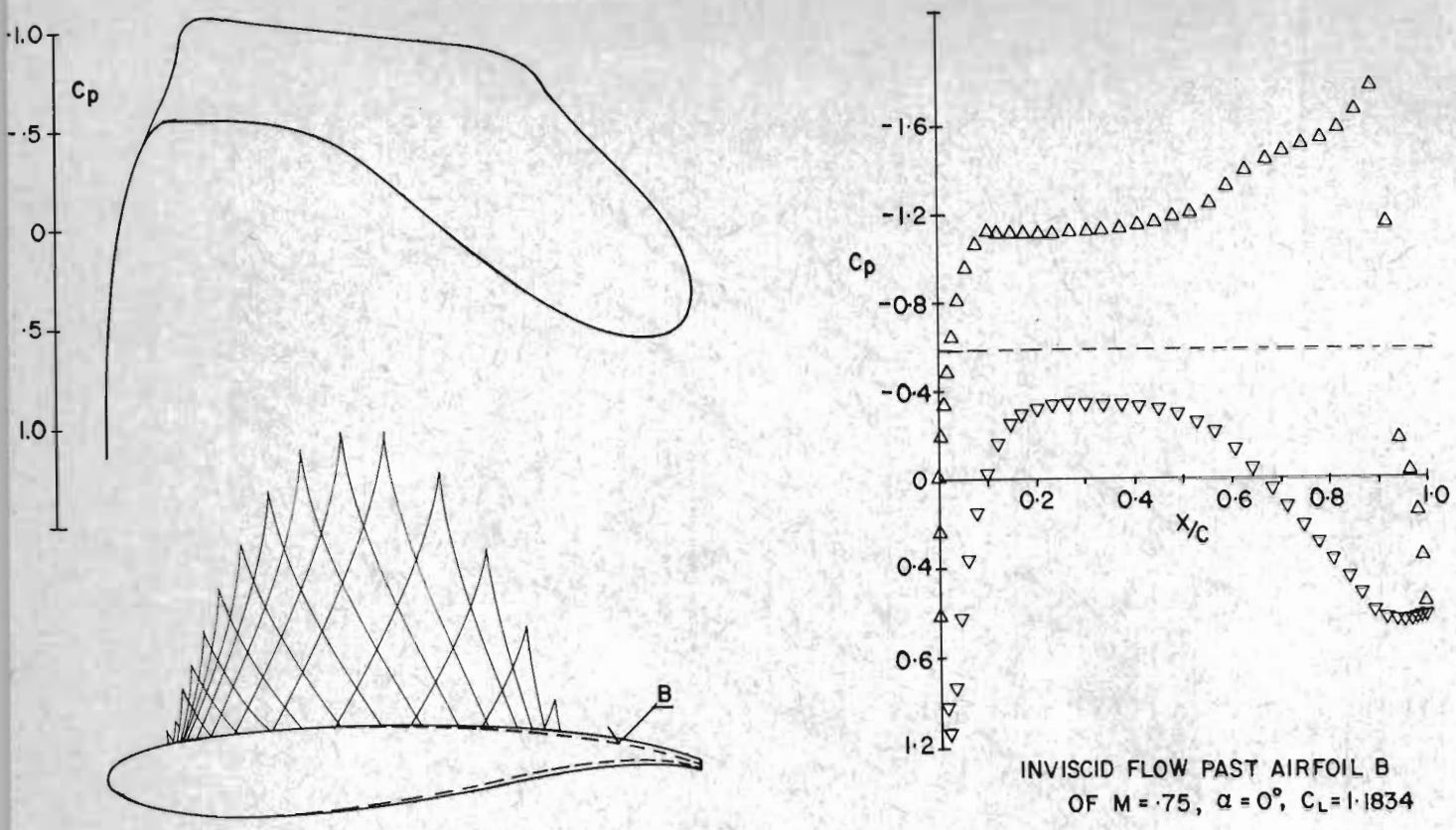

M = .75 C_L = .667 T/C = .151

FIGURE 11 SHOCKLESS LIFTING AIRFOIL II

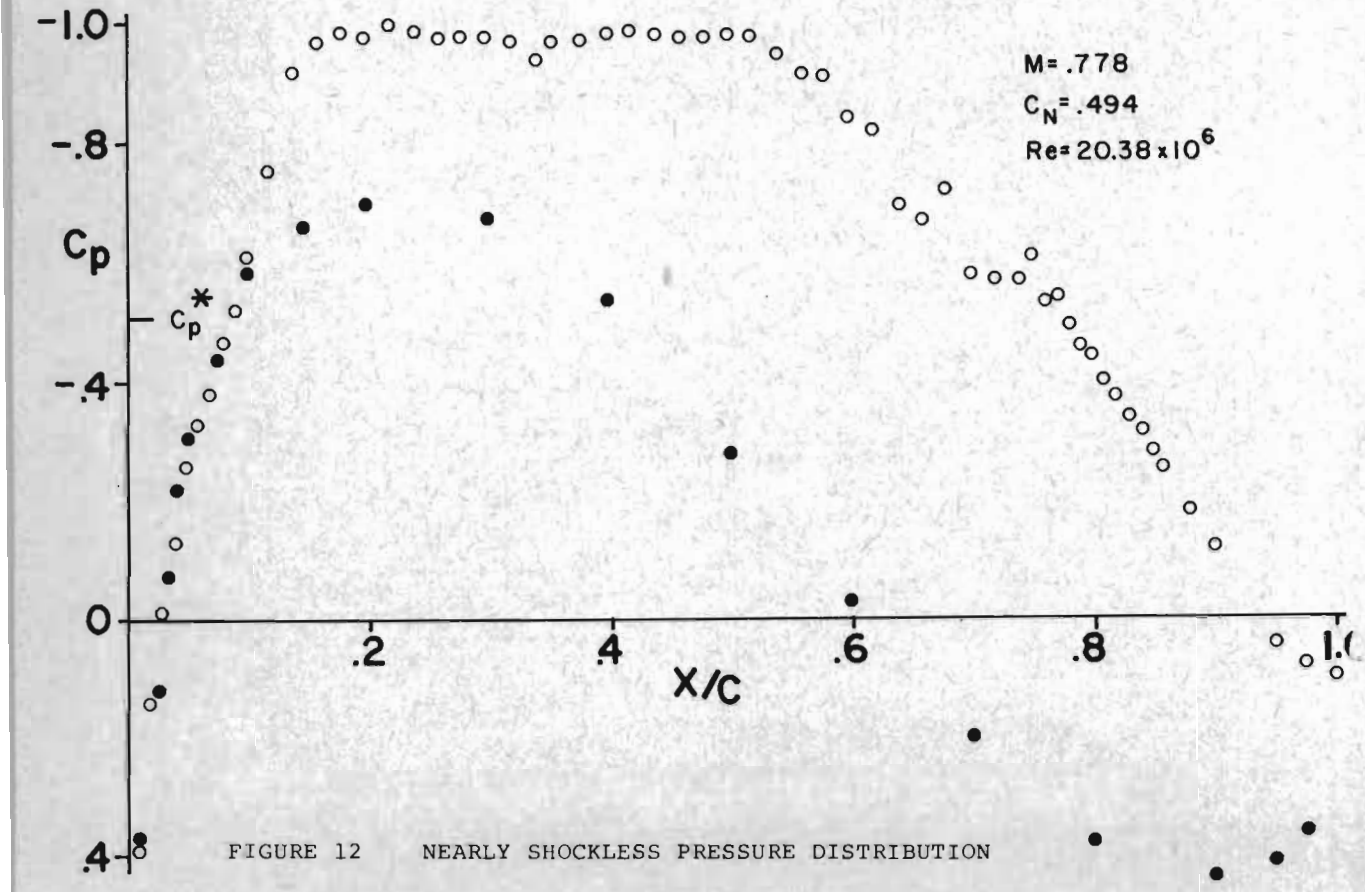

FIGURE 12 NEARLY SHOCKLESS PRESSURE DISTRIBUTION

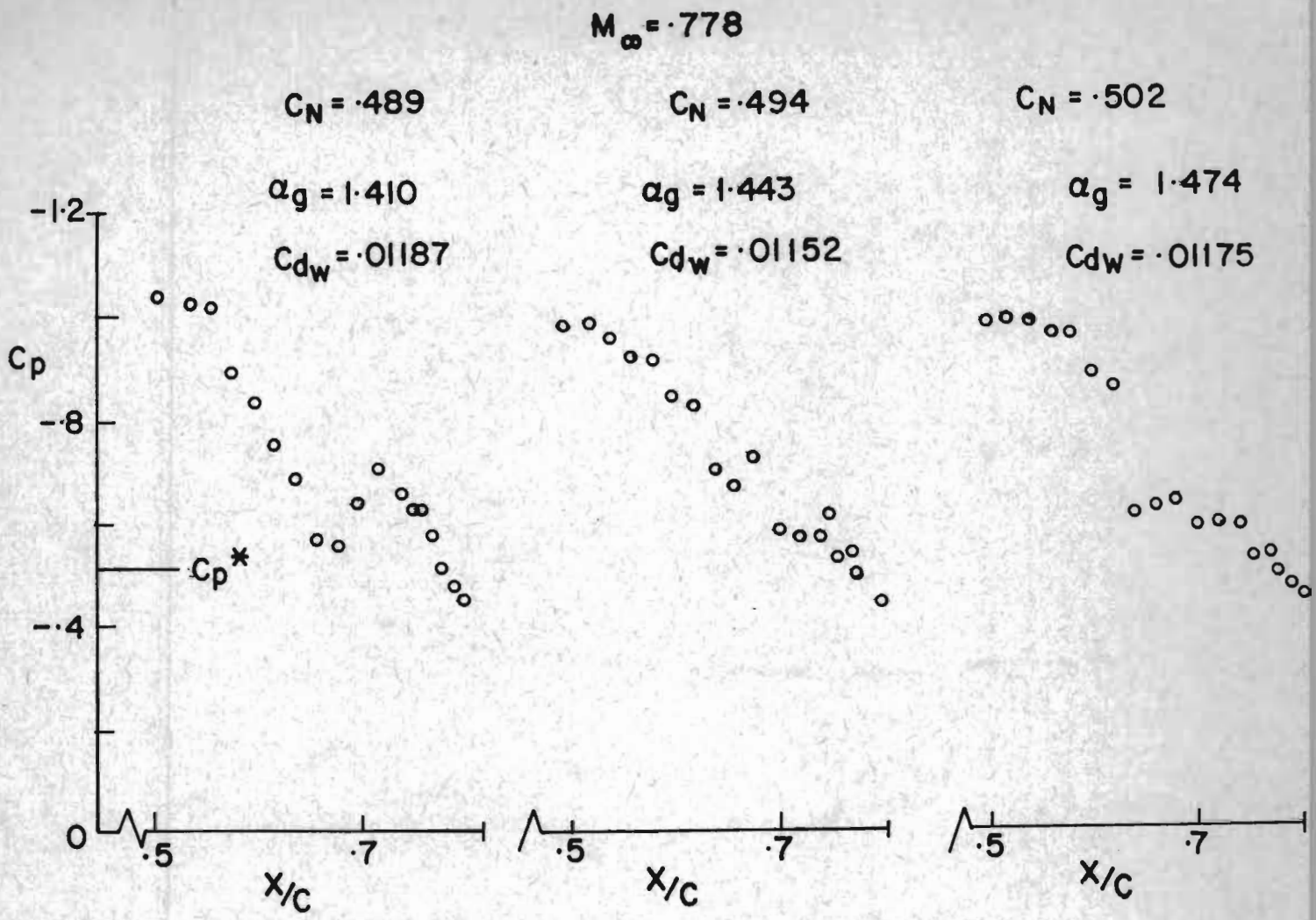

FIGURE 13 VARIATION OF NEARLY SHOCKLESS FLOW WITH ANGLE OF ATTACK

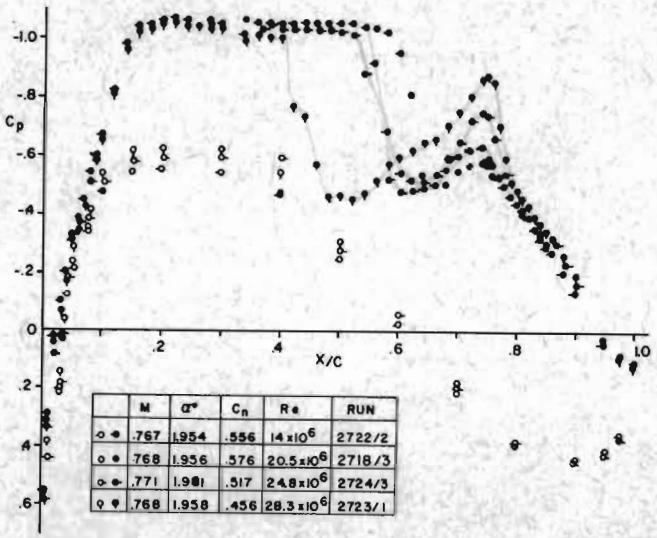

FIGURE 14 EXAMPLE OF REYNOLDS NUMBER EFFECT

FIGURE 15

INVISCID FLOW CALCULATION PAST SHOCKLESS LIFTING AIRFOIL NO.2 BETWEEN POROUS WIND TUNNEL WALL WITH POROSITY P = .355 AND FOR H/C = 6

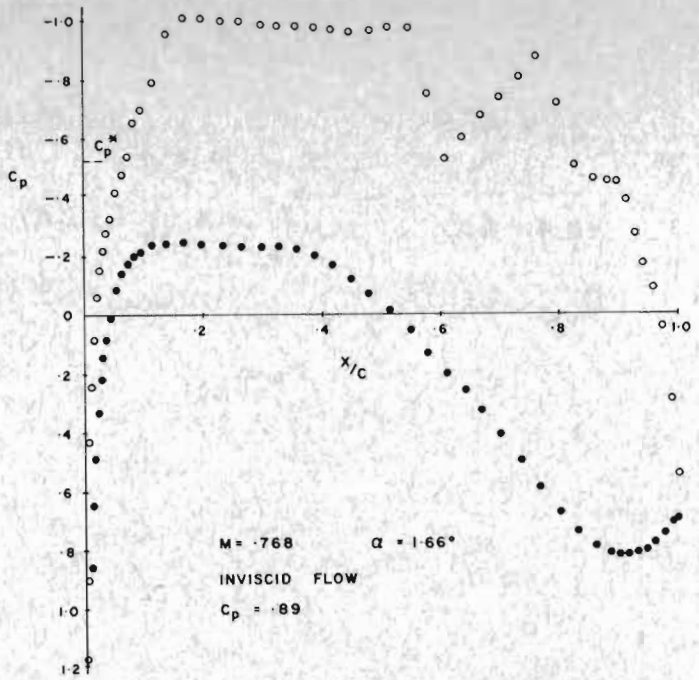

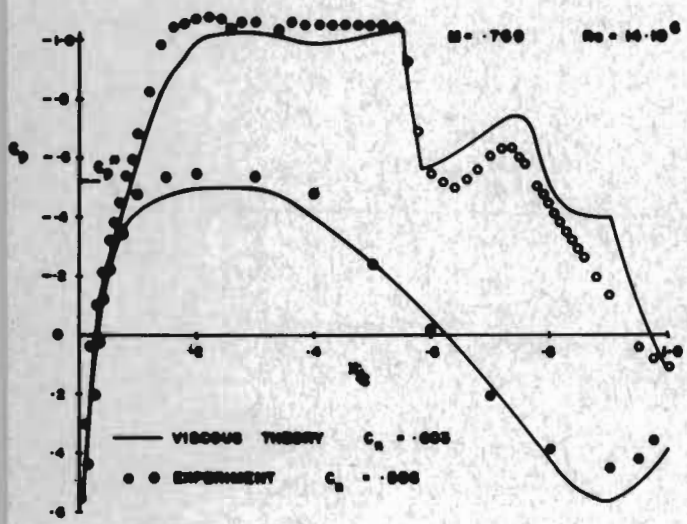

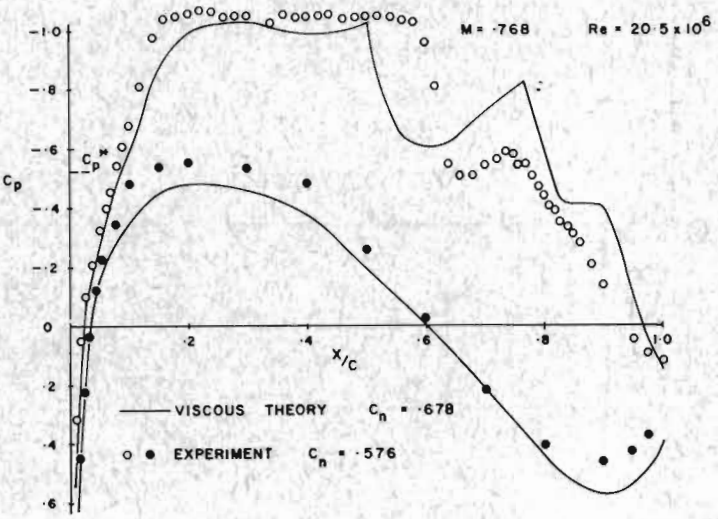

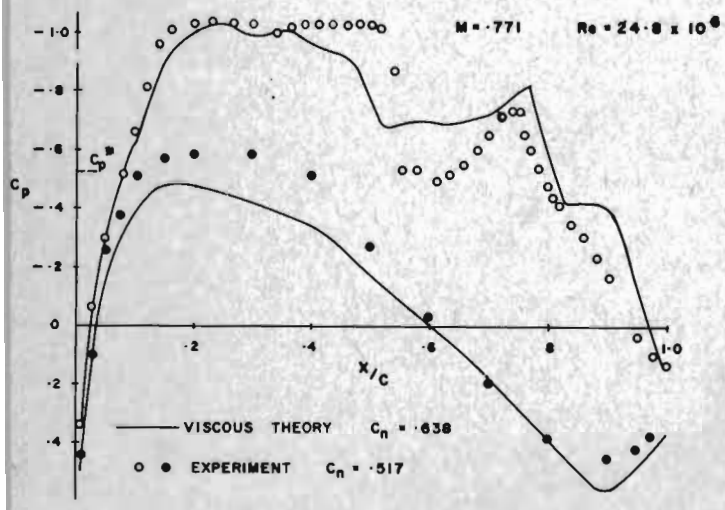

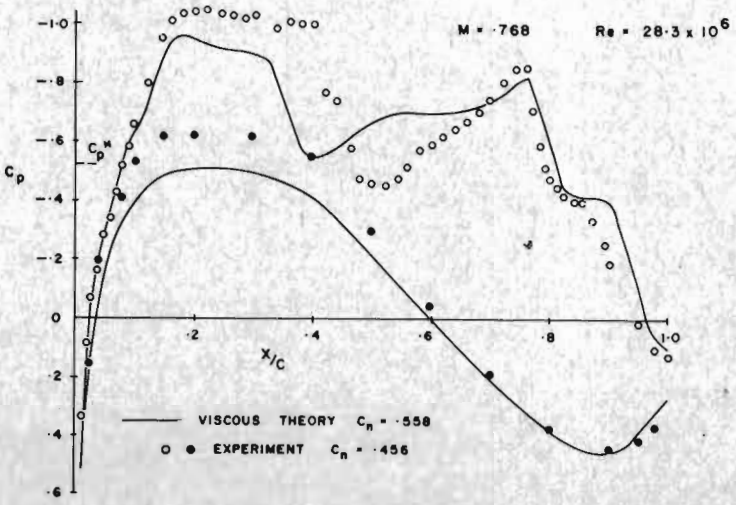

FIGURES 16 - 19 COMPARISON OF VISCOUS FLOW CALCULATION BETWEEN POROUS WALL AND EXPERIMENT

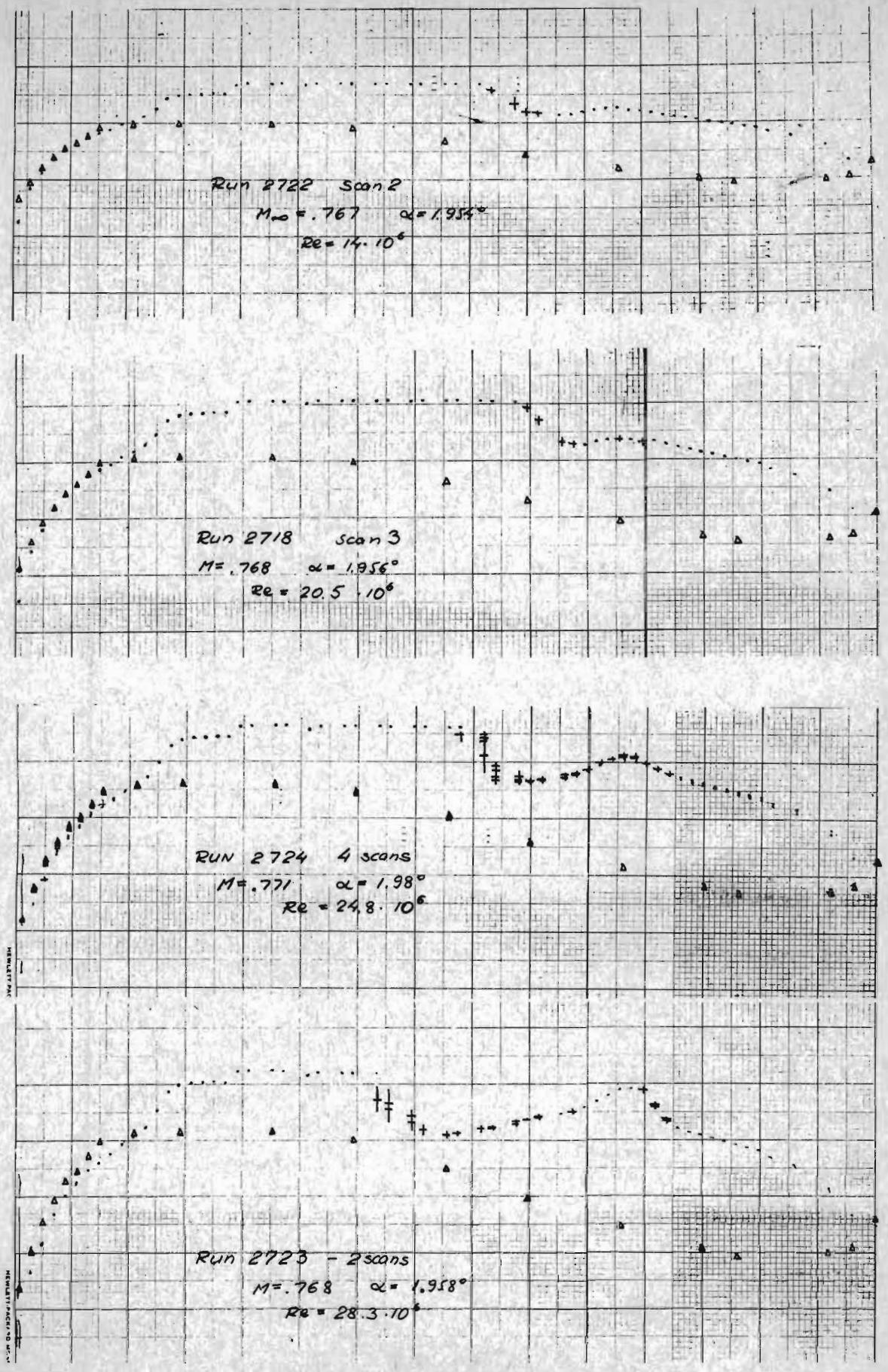

FIGURES 20 - 23 "QUICK-LOOK" RAW DATA PLOT

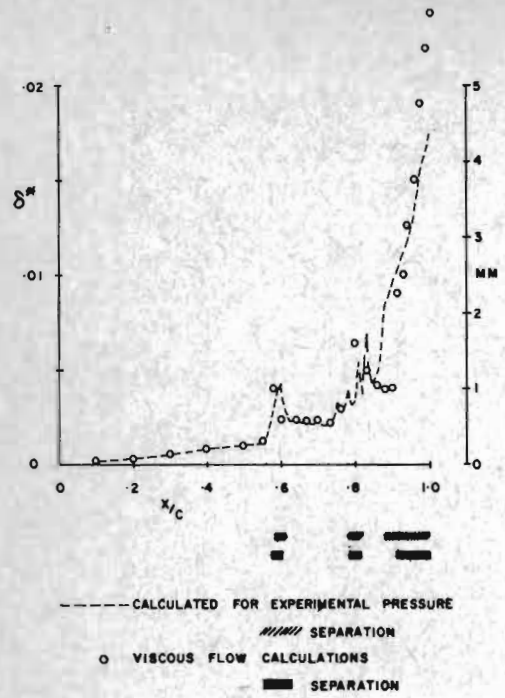

------ CALCULATED FOR EXPERIMENTAL PRESSURE

//////// SEPARATION

o VISCOUS FLOW CALCULATIONS

▬▬ SEPARATION

M = ·767 Re = 14·10^6

UPPER SURFACE

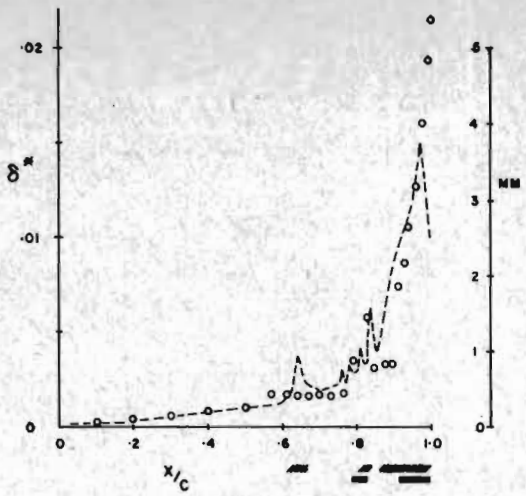

– – – – CALCULATED FOR EXPERIMENTAL PRESSURE

▬▬ SEPARATION

o VISCOUS FLOW CALCULATIONS

▬▬ SEPARATION

M = ·768 Re = 20·5 x 10^6

UPPER SURFACE

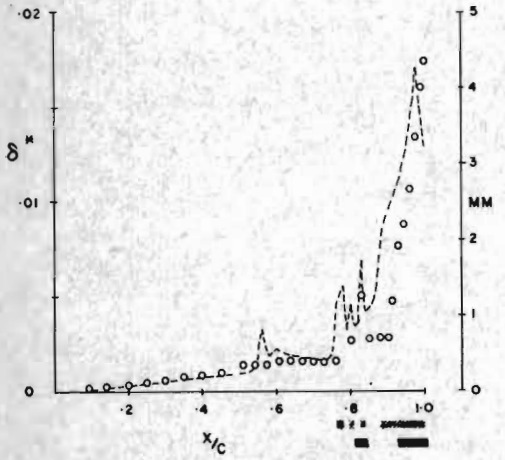

------ CALCULATED FOR EXPERIMENTAL PRESSURE

//////// SEPARATION

o VISCOUS FLOW CALCULATIONS

▬▬ SEPARATION

M = ·771 Re = 24·8 x 10^6

UPPER SURFACE

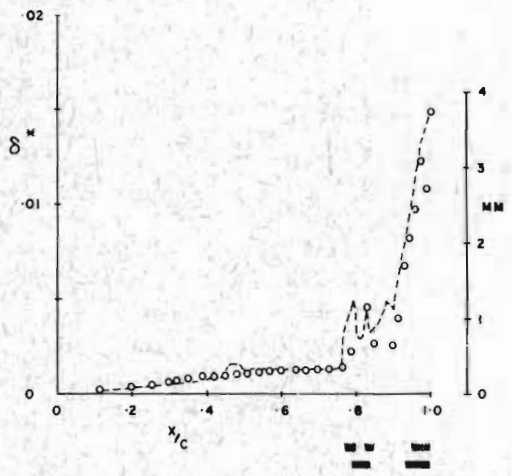

------ CALCULATED FOR EXPERIMENTAL PRESSURE

//////// SEPARATION

o VISCOUS FLOW CALCULATIONS

▬▬ SEPARATION

M = ·768 Re = 28·3 x 10^6

UPPER SURFACE

FIGURES 24 - 27 COMPARISON OF BOUNDARY LAYERS ON UPPER SURFACE

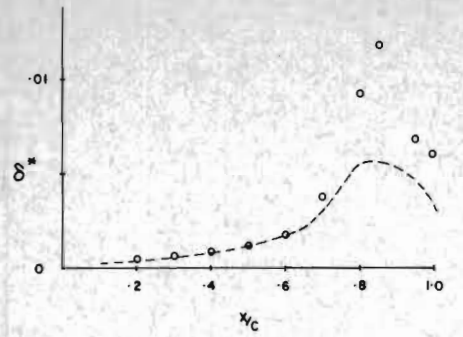

----CALCULATED FOR EXPERIMENTAL PRESSURE

o VISCOUS FLOW CALCULATIONS

M = ·767 Re = 14·10^6

LOWER SURFACE

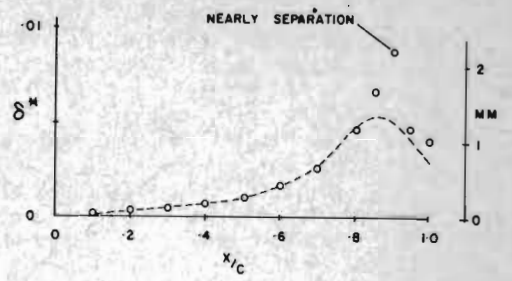

----CALCULATED FOR EXPERIMENTAL PRESSURE

o VISCOUS FLOW CALCULATIONS

M = ·768 Re = 20·5 x 10^6

LOWER SURFACE

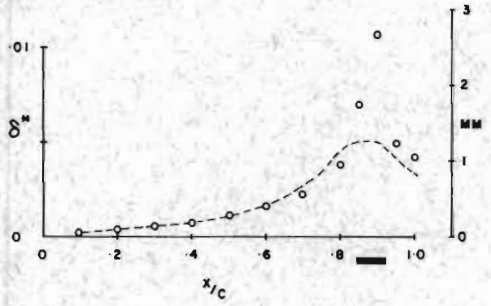

----CALCULATED FOR EXPERIMENTAL PRESSURE

o VISCOUS FLOW CALCULATIONS

▬ SEPARATION

M = ·771 Re = 24·8 x 10^6

LOWER SURFACE

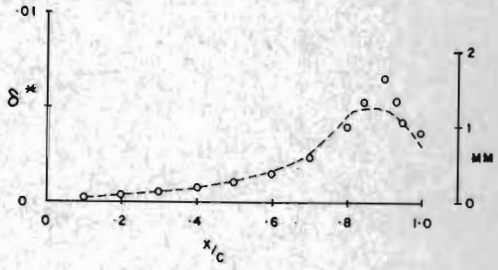

----CALCULATED FOR EXPERIMENTAL PRESSURE

o VISCOUS FLOW CALCULATIONS

M = ·768 Re = 28·3 x 10^6

LOWER SURFACE

FIGURES 28 - 31 COMPARISON OF BOUNDARY LAYERS ON LOWER SURFACE

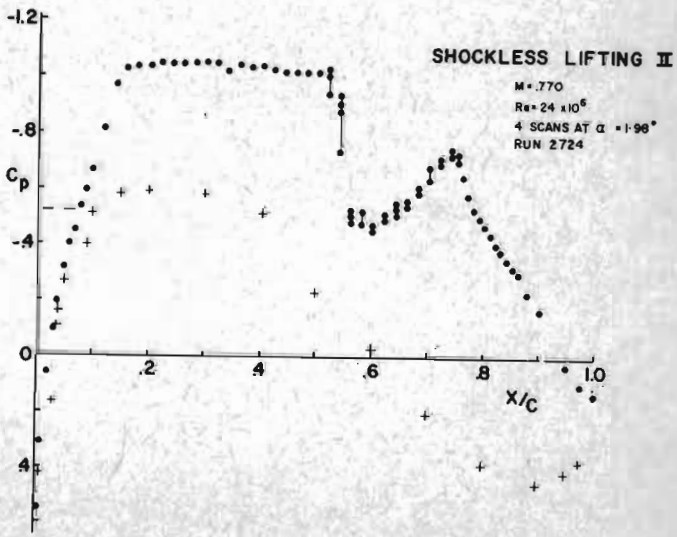

FIGURE 32

REPEATABILITY OF EXPERIMENT

D I S C U S S I O N

A. Das (DFVLR-Braunschweig, Germany) : In one picture of your paper a comparison is made of the flow field of one airfoil in free flight condition and with wind tunnel constraints having porous walls - the results indicate quite an amount of deviation. From the point of view of the correct simulation of the flow field, was the parameter of wall porosity changed to have the correct condition? It may be that a change of the porosity of the walls can lead to closure simulation.

J.J. Kacprzynski : The comparisons between a flight pressure distribution and the wind tunnel and the theoretical results were made only for a conventional airfoil NACA 651-213. This airfoil is less sensitive to the change of the flow parameters than the supercritical airfoils. The theoretical calculations of this airfoil were not performed for free flow condition (no wind tunnel wall effects) but for experimental values of the Mach number, lift coefficient and Reynolds number. In this special case both the inviscid and the viscous theoretical flow calculations agree extremely well with the wind tunnel results. The small disagreement with the flight pressure distribution is due to imperfection of the geometry of the wing section.